Particuology 36 (2018) 185–189

Contents lists available at ScienceDirect

Particuology

journal homepage: www.elsevier.com/locate/partic

Deposition of non-spherical microparticles in the human upper respiratory tract

Lixing Jia [a], Lianzhong Zhang [a,*], Suyuan Yu [b]

[a] School of Physics, Nankai University, Tianjin 300071, China
[b] Institute of Nuclear and New Energy Technology, Tsinghua University, Beijing 100084, China

ARTICLE INFO

Article history:
Received 26 November 2016
Received in revised form 21 June 2017
Accepted 28 June 2017
Available online 16 November 2017

Keywords:
Particle deposition
Non-spherical microparticles
Human upper airway
Shape factor

ABSTRACT

We investigated the deposition pattern of microparticles with different particle diameters, shape factors, and initial flow conditions in a realistic human upper respiratory tract model. We identified a close relationship between the deposition fraction and the particle shape factor. The deposition fraction of the particles decreased sharply with increasing particle shape factor because of the decreasing drag force. We also found that the deposition varied at different positions in the upper respiratory tract. At low shape factors, the highest fraction of particles deposited at the mouth and pharynx. However, with increasing shape factor, the deposition fraction in the trachea and lungs increased. Moreover, for a given shape factor, larger particles deposited at the mouth and pharynx, which indicates that the deposition fraction of microparticles in the human upper respiratory tract is affected first and foremost by particle inertia as well as by the drag force.

Introduction

The human upper respiratory tract, which consists of the nasal cavity, oral passage, nasopharynx, oropharynx, larynx, and trachea, connects ambient air and the human lungs and plays a critical role in human physical health. In addition to respiration, a fundamental function of the upper respiratory tract is to prevent fine particles from entering the lungs. A large body of both numerical and experimental research has been carried into the interaction of inhaled particles with the upper respiratory tract. For example, depositions of micro- or nanoparticles have been studied using airway replicas made from cadavers (Abouali et al., 2012; Farhadi Ghalati et al., 2012; Huang, Sun, Liu, & Zhang, 2013; Huang & Zhang, 2011; Zhang & Kleinstreuer, 2004; Zhang, Kleinstreuer, Donohue, & Kim, 2005). In another study, a human upper respiratory tract model with an idealized oral region and an asymmetric tracheobronchial airway was built (Huang, Zhang, & Yu, 2011), in which the airflow and microparticle deposition and transport was simulated. Using high-resolution computed tomography data, Islam, Saha, Sauret, Gemci, and Gu (2017) built a digital 17-generation human pulmonary airway model to study particle transport and deposition in the deep airways of the human lung. Su and Cheng (2006, 2009) carried out experiments to investigate the effects of the dimensions and inertia of fibers on the deposition pattern. The drag of both regular- and irregular-shaped non-spherical particles was investigated by several groups (Bagheri & Bonadonna, 2016; Loth, 2008; Mando & Rosendahl, 2010), leading to the development of a new formula and measurements of shape-dependent drag correlations (Dioguardi & Mele, 2015; Krueger, Wirtz, & Scherer, 2015). Dastan, Abouali, and Ahmadi (2014) performed computational fluid dynamics simulations of the deposition of fibrous particles in different realistic human nasal cavities. Finally, Dogonchi, Hatami, Hosseinzadeh, and Domairry (2015) used a Pade approximate to study the velocity and acceleration of non-spherical particles in incompressible Newtonian media.

In this paper, based on a more refined human upper respiratory tract model than that constructed by Huang et al. (2011), we investigated the movement and deposition of non-spherical microparticles using a particle shape factor. Particles of two different diameters (1 and 2.5 μm) and three kinds of inspiratory conditions were chosen. Moreover, we studied both the total and regional aerosol deposition.

* Corresponding author.
E-mail address: zhanglz@nankai.edu.cn (L. Zhang).

https://doi.org/10.1016/j.partic.2017.06.009

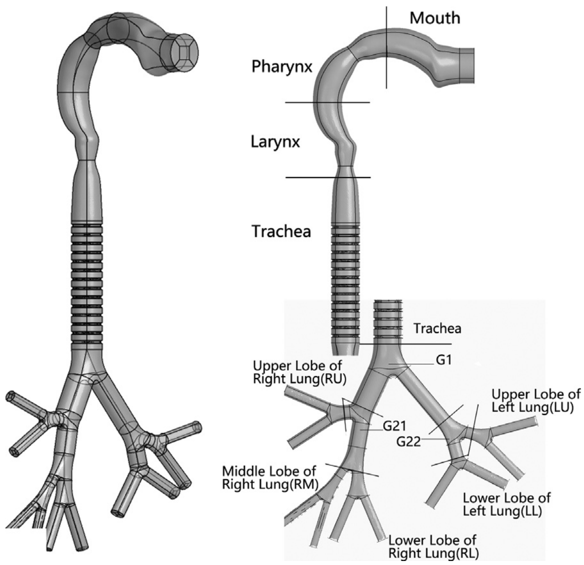

Fig. 1. Schematic representation of the human upper respiratory tract model.

Numerical model

Geometry

As shown in Fig. 1, the human upper respiratory tract model consists of two parts: an oral airway region, including the oral cavity, pharynx, larynx, and trachea, and an asymmetric bronchial airway including four generations and five lung lobes. The oral airway model was built from a realistic human replica (Cheng, Zhou, & Chen, 1999), which was validated by Huang et al. (2011) and Zhang, Kleinstreuer, and Kim (2002). The governing equations include the Reynolds-averaged Navier–Stokes equations, which can be expressed as the continuity equation,

$$\frac{\partial \bar{u}_i}{\partial x_i} = 0, \tag{1}$$

and the momentum equation,

$$\frac{\partial \bar{u}_i}{\partial t} + \partial \bar{u}_j \frac{\partial \bar{u}_i}{\partial x_j} = -\frac{1}{\rho}\frac{\partial \bar{p}}{\partial x_i} + \frac{\partial}{\partial x_i}\left((\nu + \nu_t) + \left(\frac{\partial \bar{u}_i}{\partial x_j} + \frac{\partial \bar{u}_j}{\partial x_i}\right)\right), \tag{2}$$

where $\bar{u}_i$, $\bar{u}_j$ are the averaged velocity vector of the x, y, z components with $i, j = 1, 2, 3$, ρ is the fluid density, $\bar{p}$ is the modified pressure, and ν and ν_t are the kinetic viscosity and turbulence kinetic viscosity, respectively. The low-Reynolds-number k–w turbulence model was adopted to simulate the airflow field in the model. The turbulence kinetic energy (k) equation is expressed as:

$$\frac{\partial k}{\partial t} + \partial \bar{u}_j \frac{\partial k}{\partial x_j} = \tau_{ij}\frac{\partial \bar{u}_i}{\partial x_j} - \beta' k\omega + \frac{\partial}{\partial x_j}\left((\nu + \sigma_k \nu_T)\frac{\partial k}{\partial x_j}\right), \tag{3}$$

and the pseudo-vorticity (ω) equation is expressed as:

$$\frac{\partial \omega}{\partial t} + \partial \bar{u}_j \frac{\partial \omega}{\partial x_j} = \tau_{ij}\frac{\partial \bar{u}_i}{\partial x_j} - \beta\omega^2 + \frac{\partial}{\partial x_j}\left((\nu + \sigma_\omega \nu_T)\frac{\partial \omega}{\partial x_j}\right), \tag{4}$$

where τ_{ij} is the Reynolds stress tensor, and α, β, β', σ_k, and σ_ω are turbulence constants ($\alpha = 0.555$, $\beta = 0.75$, $\beta' = 0.09$, and $\sigma_k = \sigma_\omega = 2$).

Particle transport

Microparticle transport in the human upper respiratory tract model is considered to behave as a dilute, monodisperse, rigid-sphere suspension, with negligible rotation and a large

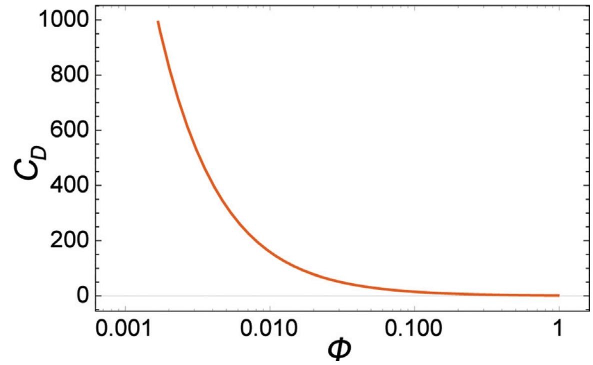

Fig. 2. Drag coefficient (C_D) as a function of sphericity (Φ) for a Reynolds number of 100.

particle-to-air density ratio. In this case, the drag force is dominant, based on order-of-magnitude arguments. Hence, the particle trajectory equation can be written as:

$$m_p \frac{d\mathbf{u}^p}{dt} = \frac{1}{8}\pi\rho d_p^2 C_{Dp}|\mathbf{u} - \mathbf{u}^p|(\mathbf{u} - \mathbf{u}^p), \tag{5}$$

where m_p, u_i^p, and d_p are the spherical particle mass, velocity vector, and diameter, respectively. C_{Dp} is the drag force coefficient given by,

$$C_{Dp} = \frac{C_D}{C_{slip}}, \tag{6}$$

where

$$C_D = \max\left(\frac{24}{Re_p}\left(1 + 0.15Re_p^{0.678}\right), 0.44\right), \tag{7}$$

and where $Re_p = |\mathbf{u} - \mathbf{u}^p| d_p/\nu$ is the particle Reynolds number, and C_{slip} is a correlation for the Cunningham correction factor.

Drag of non-spherical particles

For non-spherical particles, there are many correlations based on different models for estimating the drag coefficient. A correlation formula for the drag coefficient was established by Hölzer and Sommerfeld (2008) given by,

$$C_D = \frac{8}{Re}\frac{1}{\sqrt{\Phi_\parallel}} + \frac{16}{Re}\frac{1}{\sqrt{\Phi}} + \frac{3}{Re}\frac{1}{\sqrt{\Phi^{3/4}}} + 0.42 \times 10^{0.4(-\log\Phi)^{0.2}}\frac{1}{\Phi_\perp}, \tag{8}$$

where Re is the Reynolds number of the particle, Φ is the particle sphericity (defined as the ratio of the surface area of a spherical particle with the same volume as the non-spherical particle to the surface area of the non-spherical particle), $\Phi_\perp$ is the crosswise sphericity (defined as the ratio of the projected area of an equivalent-volume sphere to the projected area of the considered particle), and $\Phi_\parallel$ is the lengthwise sphericity (defined as the ratio between the cross-sectional area of an equivalent-volume sphere to the difference between half the surface area and the mean projected longitudinal cross-sectional area of the considered particle). The orientation of the particle is also considered to obtain the drag coefficient. Because the evaluation of $\Phi_\parallel$ is complex, its replacement has been suggested, at the cost of a slight reduction in accuracy (Hölzer & Sommerfeld, 2008). For the calculation of both $\Phi_\parallel$ and $\Phi_\perp$, it is necessary to know the orientation of the particle; thus, it is more suitable to use Eq. (8) for Lagrangian computations where the paths of the particles are known. Using Eq. (8), we determined the pattern of C_D and compared the correlation of the deposition fraction of the particles and the particle shape factor. These results are shown in